THE INFLUENCE OF MICROSTRUCTURE AND STRESS RATIO ON FATIGUE CRACK GROWTH IN WC-Co HARDMETALS

N. Knee and W. J. Plumbridge

Department of Mechanical Engineering, University of Bristol, Bristol BS8 1TR, England

ABSTRACT

Fatigue crack growth tests on five grades of WC-Co hardmetal, typical of those used in the mining industry, are described. At intermediate growth rates the Paris equation ($da/dN = A\Delta K^m$) applies, with the value of m increasing with decreasing cobalt content and WC grain size. The effects of fracture toughness, microstructure and stress ratio on fatigue crack growth rates are discussed. A microstructure independent threshold for crack propagation is observed and the concept of crack closure is used to explain the effect of stress ratio on this threshold. Detailed examination of the fatigue crack path gives an insight into the mechanisms of fatigue crack advance which, it is proposed, involves the brittle fracture of WC grains ahead of the crack tip, followed by failure of the Co ligaments.

KEYWORDS

Fatigue crack growth; fracture toughness; WC-Co hardmetals; microstructure; crack closure.

INTRODUCTION

The hardmetals used for cutting tool tips in the mining industry are generally made by sintering a mixed powder of finely-divided tungsten carbide (WC) and cobalt (Co). The resultant microstructure is a composite of very hard WC grains in a Co-rich matrix with a small amount of residual porosity. Under certain conditions, particularly when cutting softer low-abrasive minerals, such as coal, the tool tip develops a network of fine cracks, which are usually attributed to thermal fatigue. Tool failure during drilling of hard low-abrasive minerals is also thought to be a result of impact/fatigue. In this paper, an investigation of the growth of fatigue cracks in hardmetals under mechanical loading at ambient temperatures in air is described. The objective is to quantify crack growth rates and to identify the microstructural parameters which influence fatigue crack growth. Such information will aid understanding of the mechanisms of failure.

EXPERIMENTAL DETAILS

Fatigue tests were carried out on five grades of hardmetal using rectangular section specimens, 40 mm long, 4 mm thick and 8 mm wide. The specimens were supported on 5 mm diameter sintered alumina rollers, and loaded in four point bending at a frequency of about 80 Hz in an Amsler "Vibrophore". This geometry was selected because of the ease of manufacture, because the stress intensity factor, K is well known, and because a fairly straight crack front can be produced. Earlier shortcomings regarding unstable crack propagation in brittle materials with this geometry (Evans, 1974) have been discounted (Almond and Roebuck, 1980).

Crack length was measured using the DC potential drop method and the fatigue cracks were initiated from spark machined slots about 2 mm deep and 0.3 mm wide, with a root radius of 0.15 mm. Microcracking at the tip of the slot caused by the spark-machining was found to facilitate initiation. After a crack had been initiated, the load was stepped down by increments until a low crack growth rate was achieved. The remainder of the test was carried out at constant load amplitude. Tests were carried out at stress ratios (R) of 0.1 and 0.5, where R is defined as the ratio of minimum stress to maximum stress in a fatigue cycle. The test was stopped after about 2 mm of crack extension when the crack growth rate was $\simeq$ 0.1 μm/cycle. After fatigue testing, a fracture toughness test was carried out on each specimen. The K_{IC} test procedure followed British Standard 5447 (1977), although for some tests the final fatigue load was in excess of 0.7 K_{IC}, as the standard requires. In view of the limited plasticity in hardmetals, it was felt that this would not seriously affect the results.

The microstructures of all the grades tested were quantified using either scanning electron micrographs or transmission electron micrographs of shadowed carbon replicas taken from specimens etched in Murakami's reagent. The use of optical micrographs for the quantification of fine-grained hardmetals has been shown to result in systematic errors (Exner and Fischmeister, 1966). Lineal analysis was used to evaluate the important microstructural parameters and to obtain the grain size distribution. Measurements were obtained of the volume fraction of binder, f, the mean grain diameter, $\bar{d}$, the mean free path in the binder, λ, and the contiguity, C, which is a measure of the degree of connectivity of the WC.

RESULTS

Fatigue Crack Growth and Fracture Toughness

The crack length (a) versus number of cycles (N) data were analysed using the secant method and the results are plotted on log scales as a function of the range of stress intensity factor (ΔK) in Fig. 1 for R = 0.1 and R = 0.5. At low crack growth rates there is a threshold value of ΔK below which crack growth does not occur, and at high crack growth rates, as the maximum stress intensity in the cycle, K_{max}, approaches K_{IC}, there is an upturn in the plot of log (da/dN) v. log (ΔK). Straight lines have been fitted to the intermediate range data, to express the results in the form

$$\frac{dA}{dN} = A(\Delta K)^m \qquad (1)$$

The values for the constants in this equation, which is the well known

"Paris" law (Paris and Erdogan, 1963) are given in Table 1 together with the measured values for the hardness and fracture toughness of the materials and the nominal specification.

TABLE 1 Nominal Specification and Measured Properties for the Grades of Hardmetal Tested

Hardmetal Grade		CH	CM	BP1	TT	CXT
Nominal Grain Size (μm)		1.4	1.4	1.8	1.4	4.0
Wt% Cobalt		7.5	9.5	15	25	9.5
Measured Hardness (HV_{50})		1424	1384	1100	871	1183
K_{IC} (MPa $\sqrt{m}$)		11.8	16.3	19.2	21.4	17.3
m	R = 0.1	10.8	9.2	7.3	5.0	6.7
A(μm/cycle)	R = 0.1	2×10^{-13}	1.6×10^{-12}	2×10^{-10}	4×10^{-8}	8×10^{-10}
m	R = 0.5	24	11.6	8.8	3.9	6.5
A(μm/cycle)	R = 0.5	10^{-21}	3×10^{-12}	6×10^{-11}	1.3×10^{-6}	5×10^{-9}

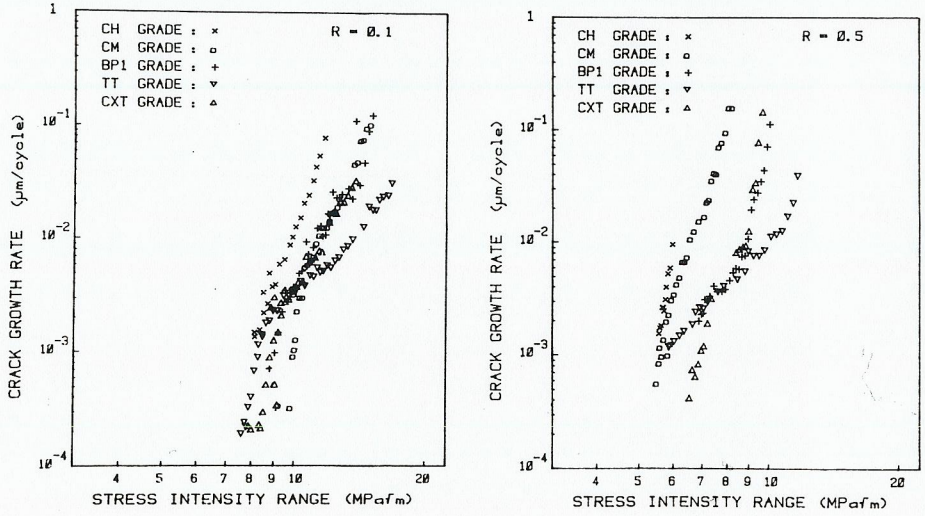

Fig. 1. Crack growth rate versus ΔK for stress ratios of R = 0.1 and 0.5.

At low stress ratios (R = 0.1) the values of the exponent m lie in the range $5 < m < 10.8$, and there is a general trend for m to increase with decreasing toughness and cobalt content, and increasing hardness. Increasing grain size decreases the value of m for a given value of toughness or cobalt content. At higher stress ratios (R = 0.5), the fatigue crack growth rates are increased and there is a wider range of values for m ($3.9 < m < 24$). The trend of m increasing with decreasing toughness is again apparent. A comparison of the data for CM and CXT grades, which have the same composition but different grain sizes shows that increasing the grain size improves the crack growth resistance. Increasing the stress ratio from R = 0.1 to R = 0.5 decreases the stress intensity range required for a given crack growth rate for all the grades tested. Values of m as a function of K_{IC} are plotted in Fig. 2.

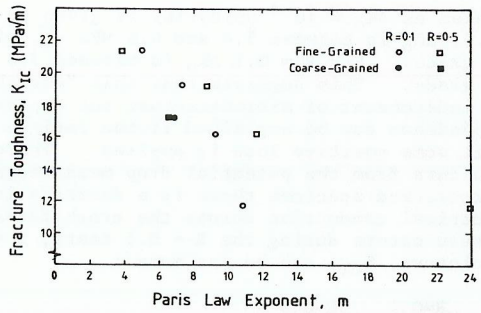

Fig. 2. Variation of toughness with Paris exponent, m.

The fracture toughness values reported are the mean of at least four tests. When the crack growth rate reached ∿ 0.1 μm/cycle, K_{max} is approaching K_{IC} and fast fracture will occur if the fatigue test is not interrupted. The values for K_{IC} lie within the scatter band of published results for similar grades of WC-Co. K_{IC} increases with increasing cobalt content for grades of similar grain size, and increases with increasing grain size for constant cobalt content. K_{IC} also increases with decreasing hardness.

Metallography

The microstructural parameters obtained from the quantitative metallography are given in Table 2, and the cumulative grain size distribution is shown in Fig. 3. Four of the grades have a fine nominal grain size and a range of cobalt contents, and there is one coarse-grained grade. The mean grain diameter was calculated from the number of grains per unit volume. The lineal measurements of chords were corrected for the effects of sectioning using the procedure developed by Spektor (1950) as described by Underwood (1970). The weight percentage of Co was calculated from the volume fraction of binder, f. The results agreed reasonably well with the specified cobalt contents shown in Table 1, considering that only a small sample of material was examined. Mean free path in the binder, λ, increases with increasing cobalt content for constant grain size, and increases with grain size for constant cobalt content.

TABLE 2 Quantitative Metallography Results

Grade	CH	CM	BP1	TT	CXT
Volume fraction of binder, f.	0.126	0.154	0.247	0.384	0.152
Weight % Co	7.6	9.4	15.7	26.7	9.3
Mean grain diameter $\overline{d}$(μm)	1.01	0.74	1.08	0.89	3.05
Mean free path, λ, (μm)	0.33	0.29	0.54	0.83	1.18
Contiguity, C.	0.57	0.56	0.33	0.31	0.63

The fatigue fracture path and fracture appearance in the coarse grained CXT grade were studied in the SEM. Figure 4 shows part of a fatigue crack and indicates remarkably little opening of the crack, even some distance back

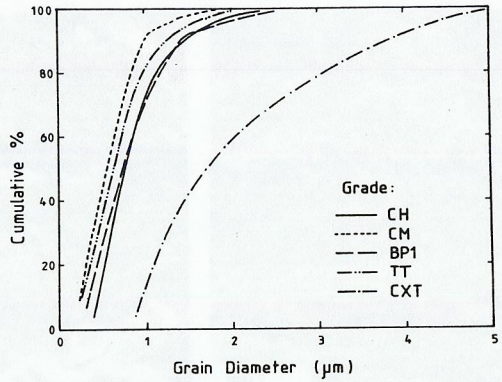

Fig. 3. Cumulative grain size distributions

from the tip. The majority of the crack path is along the interface between WC and Co, and the crack deviates around WC grains to stay at this interface. Favourably oriented WC grains in the path have been fractured and the crack also propagates across regions of binder. Figure 5 shows damage, in the form of fractured WC grains, ahead of the crack tip. There is a considerable accumulation of debris on the fatigue fracture surface (Fig. 6), especially at low stress ratios, which obscures any detail of the fracture mode in the binder. This debris is probably generated by attrition of the mating crack faces in the wake of the crack.

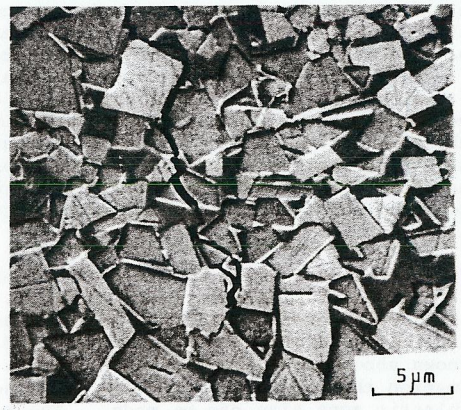

Fig. 4. Fatigue fracture path in CXT grade, about 0.1 mm from crack tip

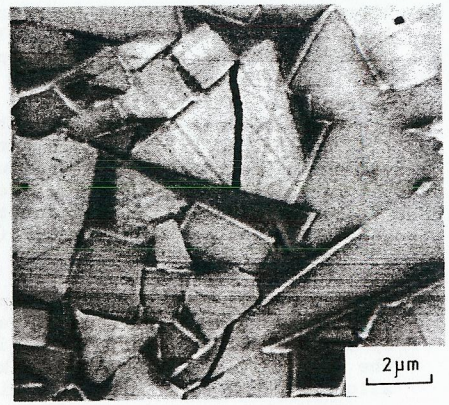

Fig. 5. Fractured WC grains about 10 μm ahead of the fatigue crack tip in CXT grade

It is not possible to distinguish between fractured WC grains and fractured WC-Co interfaces from the fatigue fracture appearance. Figure 7 shows fast fracture in the same grade, and the main difference between this and the fatigue fracture surface is the absence of debris revealing evidence of ductile rupture in the binder.

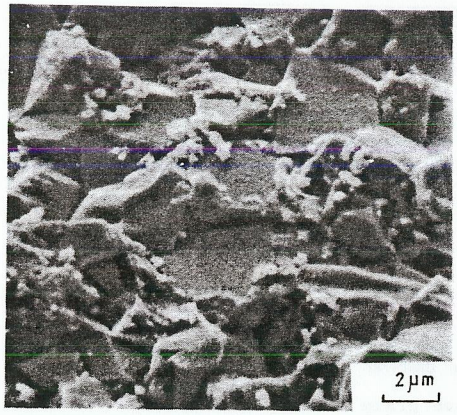

Fig. 6. Fatigue fracture in CXT grade with R = 0.1

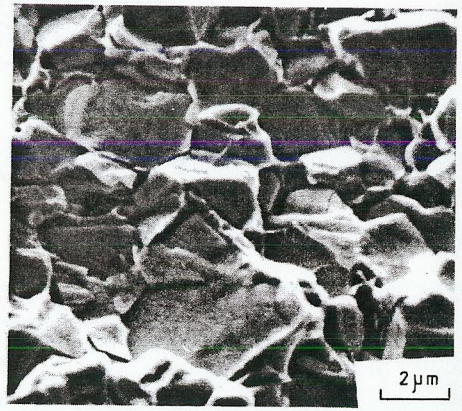

Fig. 7. Fast fracture in CXT grade

DISCUSSION

When data for ductile metals are fitted to a Paris law, the value of m usually lies in the range $2 < m < 4$. The occurrence of higher values indicates that additional "static" mechanisms such as cleavage or microvoid coalescence are contributing to the crack growth. The majority of the plastic deformation will be accommodated in the lower strength, more ductile binder phase, even though its yield strength will be raised by the constraint of the extremely hard, high modulus WC (Butler, 1972; Murray, 1976). There still remains some uncertainty about fracture paths during static fracture, but the consensus in the literature is that failure is either through the Co, or at Co-WC interfaces in fine grained alloys, with an increasing proportion of transgranular cleavage of WC in coarse grained alloys (Murray, 1976; Lueth, 1972). The fatigue fracture path (Fig. 4) shows the same elements that are observed during fast fracture, suggesting that fatigue crack propagation proceeds by increments of static fracture. The presence of fractured carbides ahead of the crack tip is consistent with the model for monotonic fracture proposed by Pickens and Gurland (1978).

For similar grain-sized alloys m increases with decreasing cobalt content (and hence decreasing mean free path, λ, and increasing contiguity, C). As λ decreases and C increases a greater proportion of the load will be carried by the carbide skeleton, increasing the likelihood of WC cleavage ahead of the crack tip. Very little is known about the extent of plasticity in WC-Co alloys, but if as a first approximation the material is assumed to be homogeneous, then an estimate of the plastic zone size can be made. The maximum extent of the zone in plane strain (Tracey, 1971) is given by $r = 0.157(K/\sigma)^2$. If the yield strength, σ, is estimated from the hardness ($\sigma \simeq 3.3$ Hv), this gives a plastic zone in CXT grade which extends about 1 μm for a stress intensity factor of 10 MPa$\sqrt{m}$. In fatigue the extent of plasticity will be about a quarter of this (Rice, 1967), so that for $\Delta K = 10$ MPa $\sqrt{m}$, the cyclic plasticity is likely to be contained within the layer of binder in which the crack tip resides.

A comparison of ΔK in the cycle for a near-threshold crack growth rate

(arbitrarily taken as $\Delta K_o = 10^{-3}$ μm/cycle) is given in Table 3, and shows that for R = 0.5, ΔK_o is between 5.4 and 6.6 MPa $\sqrt{m}$, with no systematic variation with grade. For R = 0.1, ΔK_o is between 7.6 and 9.1 MPa $\sqrt{m}$, again independent of grade. This suggests that this "threshold" stress intensity range, ΔK_o, is independent of microstructure but depends on stress ratio. The R-ratio dependence can be explained if the fatigue crack does not become fully open until some positive load is applied. There is evidence that such crack closure occurs from the potential drop measurements. During unloading of a fatigue precracked specimen there is a decrease in the p.d. caused by additional electrical conduction across the crack faces. Assuming that negligible closure occurs during the R = 0.5 tests, a value of the stress intensity for closure, K_{cl}, can be estimated:

$$K_{cl} = K_{max}^{R=0.1} - \Delta K_o^{R=0.5} \qquad (3)$$

Values for K_{cl} are given in Table 3, and lie between 2.5 and 4.7 MPa $\sqrt{m}$.

TABLE 3 Near-Threshold Fatigue Data

		CH	CM	BP1	TT	CXT
ΔK_o (MPa $\sqrt{m}$)	R = 0.1	7.9	9.1	8.3	7.6	8.1
K_{max} (MPa $\sqrt{m}$)	R = 0.1	8.8	10.1	9.2	8.4	9.0
ΔK_o (MPa $\sqrt{m}$)	R = 0.5	5.6	5.4	6.6	5.5	6.5
K_{max} (MPa $\sqrt{m}$)	R = 0.5	11.6	10.4	13.2	11.1	13.1
K_{cl} (MPa $\sqrt{m}$)		3.2	4.7	2.6	2.9	2.5

An effective stress intensity range ΔK^{eff} can be defined if crack closure occurs where

$$\Delta K^{eff} = K_{max} - K_{cl} \quad \text{if} \quad K_{cl} > K_{min} \qquad (4)$$

and

$$\Delta K^{eff} = \Delta K \quad \text{if} \quad K_{cl} < K_{min} \qquad (5)$$

For $da/dN = 10^{-3}$ μm/cycle, if closure occurs as described above, ΔK_o^{eff} is independent of both microstructure and stress ratio.

In terms of the model for crack advance in which fracture proceeds by cleavage of WC followed by failure of the binder, both of these processes must occur for crack propagation to continue. As cleavage of WC grains is governed primarily by the maximum stress in the cycle, K_{max}, which varies with R, it is unlikely that WC cleavage controls the threshold. It is proposed that it is the failure of the binder by a true fatigue mechanism which is the rate-limiting step at low crack growth rates and which gives rise to a microstructure independent "threshold".

Unfortunately, the presence of debris on the fatigue fracture surface makes it difficult to see any evidence of fatigue in the binder in the SEM. However, Almond and Roebuck (1980) detected crystallographic markings and less ductility in the binder during fatigue, indicating that different fracture mechanisms are operative in fatigue and in fast fracture. The effect of microstructure on fatigue crack growth rate becomes more important as the growth rate increases. This effect can be understood in terms of the extent of the cyclic plastic zone. When this zone extends beyond a single layer of

binder, microstructural parameters such as grain size and mean free path exert a greater influence on the crack growth rate.

CONCLUSIONS

1. Fatigue crack propagation at intermediate crack growth rates follows a power law of the form $da/dN = A\Delta K^m$, with values of m and A which depend on toughness, microstructure and stress ratio. The value of m increases and A decreases with decreasing toughness and with decreasing WC grain size. Increasing the stress ratio increases the crack growth rates.

2. At high crack growth rates the maximum stress intensity factor in fatigue approaches the fracture toughness. There is a threshold value $\Delta K_o \simeq 6MPa\sqrt{m}$ below which fatigue cracks are non-propagating, which is independent of microstructure or toughness. Crack closure can be applied to explain the effects of stress ratio on the threshold value.

3. It is proposed that the mechanism of fatigue crack propagation in WC-Co hardmetals is the cleavage of WC grains ahead of the crack tip, followed by fatigue failure of the remaining Co ligaments.

ACKNOWLEDGEMENT

Financial support for this work from the Science and Engineering Research Council is gratefully acknowledged. The authors would also like to thank Dr. P. Kenny, Dr. E.D. Yardley and Dr. J. Griffiths of the Mining Research and Development Establishment, Bretby, for helpful discussions.

REFERENCES

Almond, E.A. and Roebuck,B.(1980). Met. Technol., 7, 83.
British Standard 5447 (1977) Methods of Test for Plane Strain Fracture Toughness of Metallic Materials.
Butler, T.W. (1972). Eng. Fract. Mech., 4, 487.
Evans, A.G. (1974). In Bradt,R.C.,Hasselmann, D.P.H. and Lange F.F. (eds.) Fracture Mechanics of Ceramics, 1, 17.
Exner, H.E. and Fischmeister, H.F. (1966). Praktische Metallographie, 3, 18.
Lueth, R.C. (1972). Ph.D. Thesis, Michigan State University.
Murray, M.J. (1977). Proc. R. Soc. (Lond.), A356, 483.
Paris, P and Erdogan, F. (1963). J. Basic Eng. Trans. ASME, 85, 528.
Pickens, J.R. and Gurland, J. (1978). Mater. Sci. Eng., 33, 135.
Rice, J.R. (1967). ASTM STP 415, 247.
Spektor, A.G. (1950) Zavod. Lab., 16, 173.
Tracey, D.M. (1976). J. Eng. Mater. Technol. Trans. ASME, 98, 146.
Underwood, E.E. (1970). Quantitative Sterology, Addison-Wesley.